INVESTIGATION OF LONG RADIAL PROBE ACTIVATION IN THE PSI MAIN RING CYCLOTRON

M. I. Besana*, E. Hohmann, M. Sapinski, J. Snuverink, D. Werthmüller
Paul Scherrer Institut, 5232 Villigen PSI, Switzerland

Abstract

During an inspection of a new Long Radial Probe, inserted into the Ring cyclotron only a month earlier, an activation hot spot has been identified. The nature of this hot spot has been investigated by performing measurements of the residual activation using shielded Al_2O_3:C dosimeters, 5 mm in diameter, and a portable gamma spectrometer. Monte Carlo simulations of the probe activation with various proton energies have been performed. Results show that most of the activation comes from relatively fast decaying radionuclides and therefore the residual dose drops sufficiently during the shutdown to allow for maintenance and upgrade works. Comparing the abundances of various radionuclides estimated from measured gamma spectra with simulations at various proton energies we conclude that the most probable loss mechanism is scattering of the protons on the upstream collimator.

INTRODUCTION

The Long Radial Probe (RRL) is a device installed in the PSI's Ring cyclotron. It measures transverse beam position and profile of all orbits by measuring the effects of interaction of the beam with a thin, moving target (carbon fibre). The measured radius extends between 2080 and 4500 mm [1].

A picture of the probe moved out of the cyclotron during the gamma spectroscopy measurement is shown in Fig. 1. The cyclotron chamber is behind the large vacuum valve on the right side of the plot. The RRL structure, here in a service box with side flanges open, is normally manually inserted into the cyclotron before the start of the beam operation.

After 19 days of being inserted into the cyclotron the RRL had to be serviced. A routine activation measurement revealed presence of a hot spot with 1 mSv/h. Red star marks the location of this hot spot. Additional measurements performed using small Al_2O_3:C chips exposed directly to activated structure and shielded from other directions revealed that the hot spot is on the upper structure of the RRL.

MONTE CARLO SIMULATIONS

The established method for the activation calculations at PSI is the coupling of Monte Carlo simulations with the general purpose radiation transport code MCNP [2] and the nuclide inventory code FISPACT [3].

The object under study is modeled in the MCNP 6.2 geometry and it is divided in smaller cells to estimate the activation as a function of the position. Particles are transported

_____

* Ilaria.Besana@psi.ch

from the loss points to the regions of interest with MCNP. The flux of neutrons up to 20 MeV and the production rates of radionuclides are calculated in each cell of the geometry. The coupling script [4] is then used to prepare the input files for the FISPACT code, which include MCNP results and the irradiation history. The nuclide inventory of each cell at any time step is finally calculated.

The RRL device is modeled as two blocks of an aluminium-magnesium alloy called EN-AW-508, with dimensions of 1 m in the radial direction (x), 0.5 cm in the vertical direction (y) and 11.75 cm along the beam direction (z) (see Fig. 2). The distance between the two blocks in the vertical plane is 4 cm. The upper part, where higher activation has been measured, is divided in 12 cells. Cells 100-105 are between $y=2$ cm and $y=2.2$ cm, while cells 110-115 are between $y=2.2$ cm and $y=2.5$ cm. The lower part is not segmented and it is called cell 200.

Since the beam losses at the location of the RRL device are not known, some assumptions have been made for the simulations. The proton beam is moving along the z direction and it is impacting on the device front face. It is uniformly distributed over 1 m in x and between 2.0 cm and 2.2 cm in y. Twelve simulations have been performed considering the following beam energies (in MeV): 10, 20, 40, 60, 80, 100, 140, 200, 300, 400, 500, and 590.

The spectrum of the produced neutrons and the rates of residual nuclei have been calculated for each cell and used as input for the FISPACT calculations. The considered operation history is summarized in the Table 1. A constant lost current of 1 nA has been assumed for both irradiation periods. The end of the first cooling time corresponds to the moment when the hot spot was identified, while the end of the third cooling time corresponds to the time of the gamma spectra measurement.

Table 1: Part of the beam exposition history relevant for this activation study.

	Dates (2022)	Length
1st irradiation	Apr., 27th - May, 16th	19 days
1st cooling	May, 16th ev. - May, 18th	36 hours
2nd cooling	May, 18th - May, 19th	29 hours
2nd irradiation	May, 19th - June, 13th	25 days
3rd cooling	June, 14th	12 hours

For each cell, the nuclide inventory at each time step is calculated, as well as the residual dose that would be generated at 1 m by 1 g of material. The highest dose rates are always observed in cell 100.
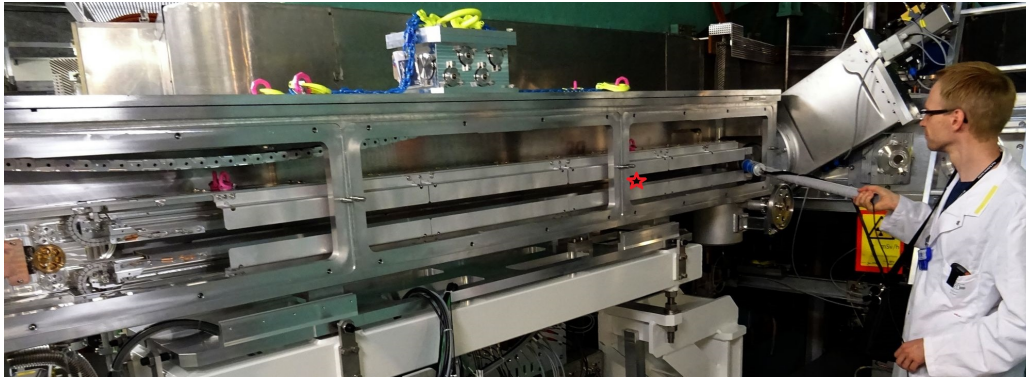
Figure 1: Gamma spectroscopy measurement of the RRL moved out of the cyclotron.
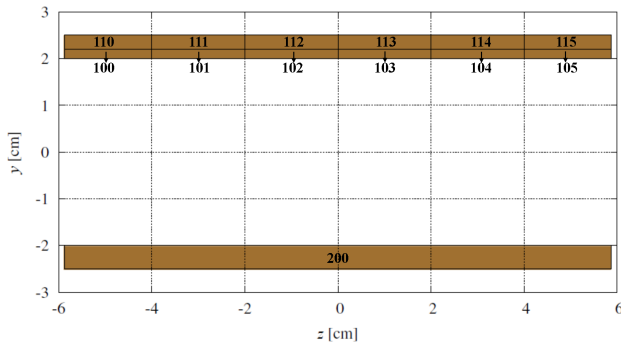

Figure 2: RRL device geometry in MCNP. The numbers in the figure correspond to the cell numbers.

For beam energies above 60 MeV, the dominant contribution comes from the decay of sodium isotopes (Na-22 and Na-24).

To calculate the residual dose to be compared with the measurements, the spectra of the gammas emitted by the radioactive nuclides and their normalisation are extracted from the output of FISPACT for each cell. The sum of the gamma spectra is used as source term for a second calculation in MCNP [5]. The expected dose map has been calculated for all proton beam energies. An example is shown in Fig. 3.
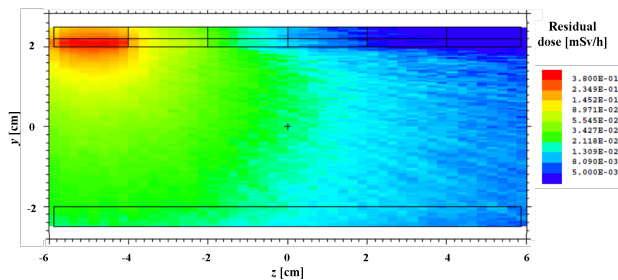

Figure 3: Residual dose map [mSv/h] at the time of the first measurement in the z-y plane, for 80 MeV proton beam and 1 nA lost current.

GAMMA SPECTROSCOPY

Several measurements of the gamma-ray energy spectrum were performed along the inner structure of the RRL (see Fig. 1). Monte Carlo simulations of the used detector were carried out in order to obtain the gamma energy distributions of various radionuclides. The sum of these distributions have then been fitted to the measured spectra to estimate the individual contributions of each of the involved nuclides.

The main region of interest is located at an orbit radius of about 230 cm, where gamma dose rate measurements revealed a radiation hot spot (see Fig. 1). A LaBr$_3$-based hand-held scintillator detector (model B-RAD by ELSE Nuclear [6]) was used to measure gamma spectra up to an energy of 2 MeV with a resolution of 3.3% (FWHM) at 662 keV. The black line in Fig. 4 shows the obtained spectrum at the location of the major hot spot.

Using the FISPACT calculations for proton energies between 20 and 200 MeV, a list of key nuclides is identified, which contribute ≥95% to the total nuclide activity for a given proton energy. Monte Carlo simulations of the B-RAD detector are carried out to obtain the individual energy distributions of these nuclides in the detector. For this purpose, a simplistic detector model (cylindrical LaBr$_3$ crystal in aluminium housing according to the B-RAD geometry) located in front of a $5 \times 5 \times 14$ cm^3 aluminium block at a distance of 1.5 cm is built using the Geant4 framework [7–9]. Radioactive decays of the key nuclides are generated homogeneously distributed within the aluminium block. The total energy deposition in the LaBr$_3$ crystal is registered and subsequently folded with the known detector resolution.

Given the energy-dependent spectra $s_i(E_\gamma)$ for each nuclide i from the Geant4 simulation, the ansatz

$$S(E_\gamma) = \sum_{\text{Nuclide } i} c_i \cdot s'_i(E_\gamma) \tag{1}$$

with properly normalized spectra $s'_i(E_\gamma)$ of nuclide i is fitted to the measured energy distribution in the range $E_\gamma = [270, 1900]$ keV using a χ^2 minimization (ROOT MINUIT package [10]) to extract the nuclide contribution coefficients c_i. Some nuclides in the previously built list of key nuclides do not show any sensitivity in the fit ($c_i \approx 0$) and are
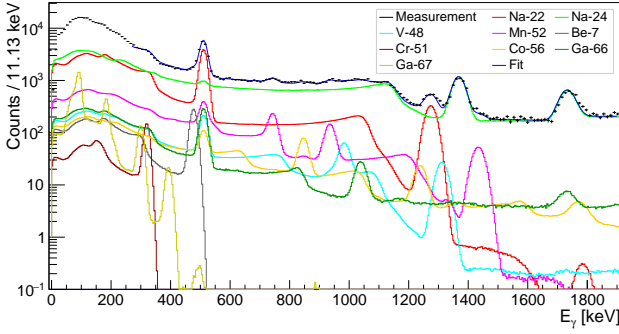
Figure 4: Measured gamma-ray energy spectrum (black points) compared to the fitted sum of simulated nuclide contributions $S(E_\gamma)$ (blue curve) and individual contributions of key nuclides.

therefore removed from the list. Figure 4 shows the measured distribution along with the fitted sum and individual nuclide contributions. The relative contributions r_i are then calculated as

$$r_i = \int_{E_0}^{E_1} c_i \cdot s_i'(E_\gamma)\, dE_\gamma \ \bigg/ \int_{E_0}^{E_1} S(E_\gamma)\, dE_\gamma \qquad (2)$$

with $E_0 = 270$ keV and $E_1 = 1900$ keV. The numerical values of r_i can be found in Table 2.

Table 2: Relative contributions r_i of key nuclides obtained from the fit of the measured gamma spectrum and from the Monte Carlo simulation (cell 100) of a 80 MeV proton beam.

Nuclide	r_i^{Fit} [%]	$r_i^{\mathrm{MC}}(80)$ [%]
Na-22	24.6 ± 0.9	30.1
Na-24	60.0 ± 1.1	58.5
V-48	2.6 ± 0.7	3.8
Mn-52	6.9 ± 0.5	5.5
Be-7	0.9 ± 0.1	0.1
Cr-51	0.3 ± 0.1	0.6
Co-56	2.3 ± 0.5	1.0
Ga-66	2.2 ± 1.0	0.2
Ga-67	0.3 ± 0.1	0.1

COMPARISON OF SIMULATED AND MEASURED NUCLIDE CONTRIBUTIONS

In order to identify the energy of the impacting protons, the relative nuclide contributions from the fit r_i^{Fit} are compared to the values $r_i^{\mathrm{MC}}(E_p)$ estimated by Monte Carlo simulations with proton energy E_p by calculating

$$\chi^2(E_p) = \sum_{\mathrm{Nuclide}\ i} \left(\frac{r_i^{\mathrm{Fit}} - r_i^{\mathrm{MC}}(E_p)}{\Delta r_i^{\mathrm{Fit}}} \right)^2 \qquad (3)$$

with uncertainties $\Delta r_i^{\mathrm{Fit}}$ originating from the spectrum fit of the key nuclides. Figure 5 shows the E_p-dependence of
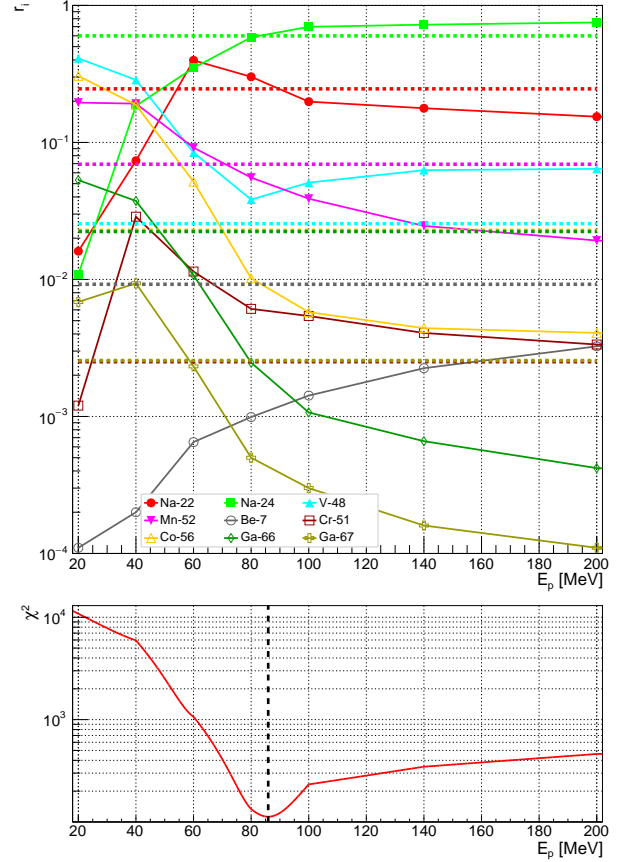

Figure 5: Top: relative nuclide contributions r_i of key nuclides obtained from measurement fit (horizontal dotted lines) and Monte Carlo simulations (solid curves) as a function of the proton energy E_p. Bottom: E_p-dependence of χ^2 with minimum at $E_p \approx 86$ MeV.

r_i^{MC} and χ^2. The latter has a minimum at $E_p \approx 86$ MeV indicating that the best agreement between measurement and Monte Carlo simulation is found at this energy.

CONCLUSIONS

A comprehensive study of the activation of the Long Radial Probe structure revealed that the observed hot spot is most likely due to protons scattered on the upstream collimator, as the best agreement between the measured and simulated gamma spectrum was found for a proton energy of $E_p \approx 86$ MeV, whereas the primary beam energy at this location is in the range of 150–180 MeV. The main radionuclide responsible for the activation is Na-24, which has a short decay time, therefore no significant buildup of the activation is expected. Nevertheless during the upcoming winter shutdown the probe will be motorized, so it will not remain inserted into the cyclotron when it is not in use.

ACKNOWLEDGEMENTS

REFERENCES

[1] M. Sapinski, R. Doelling, and M. Rohrer, "Commissioning of the renewed radial probe in PSI's ring cyclotron", in *Proc. 11th Int. Beam Instrum. Conf. (IBIC'22)*, Kraków, Poland, Sep. 2022, pp. 76–79.
`doi:10.18429/JACoW-IBIC2022-MOP19`

[2] C. J. Werner *et al.*, "MCNP6.2 Release Notes", Los Alamos National Laboratory, USA, Rep. LA-UR-18-20808, 2018.

[3] R. Forrest, "FISPACT-2007: User Manual", Technical Rep. UKAEA FUS 534, EURATOM/UKAEA, 2007.

[4] F. X. Gallmeier *et al.*, "An environment using nuclear inventory codes in combination with the radiation transport code MCNPX for accelerator activation problems", in *Proc. 8th Int. Topical Meeting on Nuclear Applications and Utilization of Accelerators (AccApp'07)*, Pocatello, ID, USA, Jul.-Aug. 2007, pp. 207-211.

[5] M. Wohlmuther and F. X. Gallmeier, "User Guide for Gamma Source Perl Script 2.0", Paul Scherrer Institut, Villigen, Switzerland, Rep. TM-85-13-05.

[6] B-RAD, ELSE Nuclear,
`http://www.elsenuclear.com/en/b-rad`

[7] S. Agostinelli *et al.*, "Geant4—a simulation toolkit", *Nucl. Instrum. Methods Phys. Res. Sect. A*, vol. 506, pp. 250–303, 2003. `doi:10.1016/S0168-9002(03)01368-8`

[8] J. Allison *et al.*, "Geant4 developments and applications", *IEEE Trans. Nucl. Sci.*, vol. 53, pp. 270-278, 2006. `doi:10.1109/TNS.2006.869826`

[9] J. Allison *et al.*, "Recent developments in Geant4", *Nucl. Instrum. Methods Phys. Res. Sect. A*, vol. 835 pp. 186–225, 2016. `doi:10.1016/j.nima.2016.06.125`

[10] R. Brun and F. Rademakers, "ROOT — An object oriented data analysis framework", *Nucl. Instrum. Methods Phys. Res. Sect. A*, vol. 389, pp. 81–86, 1997.
`doi:10.1016/S0168-9002(97)00048-X`